Low intensity repetitive transcranial magnetic stimulation drives structural synaptic plasticity in the young and aged motor cortex.

Alexander D Tang[1,2*], William Bennett[3*], Aidan D Bindoff[3], Jessica Collins[3], Michael I Garry[4], Jeffery J Summers[4,5], Mark R Hinder[4], Jennifer Rodger[1,2], Alison J Canty[3]

1. Experimental and Regenerative Neurosciences, School of Biological Sciences, University of Western Australia, Perth, Australia.
2. Perron Institute for Neurological and Translational Sciences, Perth, Australia.
3. Wicking Dementia Research and Education Centre, College of Health and Medicine, University of Tasmania, Hobart, Australia.
4. School of Psychological Sciences, College of Health and Medicine, University of Tasmania, Hobart, Australia.
5. Research Institute for Sport and Exercise Sciences, Liverpool John Moores University, Liverpool, United Kingdom

* Equal contribution

Author for correspondence: Alexander D Tang - Adtang.research@gmail.com

Abstract

Repetitive transcranial magnetic stimulation (rTMS) is a non-invasive tool commonly used to drive neural plasticity in the young adult and aged brain. Recent data from mouse models have shown that even at low intensities (0.12 Tesla), rTMS can drive neuronal and glial plasticity in the motor cortex. However, the physiological mechanisms underlying low intensity rTMS (LI-rTMS) induced plasticity and whether these are altered with normal ageing are unclear. Using longitudinal *in vivo* 2-photon microscopy, we investigated the effect of LI-rTMS on the structural plasticity of pyramidal neuron dendritic spines in the motor cortex following a single train of LI-rTMS (in young adult and aged animals) or the same LI-rTMS train administered on 4 consecutive days (in young adult animals only). We found that LI-rTMS altered the rate of dendritic spine losses and gains, dependent on the number of stimulation sessions and that a single session of LI-rTMS was effective in driving structural synaptic plasticity in both young adult and aged mice. To our knowledge, these results provide the first *in vivo* evidence that rTMS drives synaptic plasticity in the brain and uncovers structural synaptic plasticity as a key mechanism of LI-rTMS induced plasticity.

Introduction

For over three decades, repetitive transcranial magnetic stimulation (rTMS) has been used to drive neural plasticity in the human brain. Traditionally, this has been achieved by delivering transient pulses of magnetic fields over the scalp at high stimulation intensities (>1 Tesla) to drive activity within neural networks (i.e., suprathreshold stimulation). However, using rodent models, we have shown that even at low subthreshold intensities (e.g. 0.12 Tesla) that do not directly induce neuronal activity, rTMS can still induce neural plasticity. For example, we have shown that a single session of low intensity rTMS (LI-rTMS), alters neuronal excitability at the single cell (layer 5 pyramidal neurons) [1] and network level (motor evoked potentials) [2] whereas multiple sessions of LI-rTMS have been shown to promote neuronal (e.g. skilled motor learning [3]) and glial plasticity [4, 5]. However, the effect of LI-rTMS on synaptic plasticity has not, to date, been explored.

Irrespective of intensity, synaptic plasticity has long thought to be the main physiological mechanism underlying rTMS induced plasticity given the ability of rTMS to alter learning and motor evoked potential amplitudes in humans and rodents [6, 7]. In addition, synaptic plasticity is impaired in the aged brain [8-10] which in part, may explain the reports of reduced rTMS-induced plasticity in older adults [11-13]. However, despite its widespread use, the physiological mechanisms underlying rTMS induced neural plasticity remain unclear, making it difficult to determine which neurological diseases or disorders are suited for rTMS intervention. While high intensity repetitive magnetic stimulation has been shown to induce synaptic plasticity *in vitro* (organotypic hippocampal slices) [14-16], it is unknown whether high or low intensity rTMS induces synaptic plasticity *in vivo* and whether this is decreased in the aged brain.

Rodent rTMS models are a useful adjunct to human studies as they allow for direct measures of neural plasticity, including measurements of synaptic plasticity and connectivity in the living brain with longitudinal *in vivo* microscopy. Using this technique, structural plasticity of dendritic spines (the post-synaptic structure) can be quantified through changes to the density of dendritic spines and to the rates of

dendritic spine gains and losses. For example, in the motor cortex, structural synaptic plasticity is a fundamental process that facilitates the learning of skilled motor behaviours, with increases to the rate of dendritic spine gains and losses on the apical dendrites of layer 5 pyramidal neurons during the learning period [17, 18]. Using a similar longitudinal *in vivo* imaging approach, here we characterised the changes to structural synaptic plasticity in the motor cortex following a single session of LI-rTMS in young adult and "aged" mice. Additionally, we investigated whether the effects of LI-rTMS are cumulative by comparing the effects of a single day of LI-rTMS to that of multiple days of stimulation in young adult mice.

Materials and methods

Animals

Thy1-GFP-M mice (maintained on a C57BL/6J background) were used throughout, which express enhanced green fluorescent protein (EGFP) in a sparse subset of cortical excitatory neurons in layers 2/3 and 5 [19]. Mice were group housed on a 12-hour light/dark cycle and given food and water *ad libitum*. All animal experimentation was performed under the guidelines stipulated by the University of Tasmania Animal Ethics Committee (approval number: A0013168), which is in accordance with the Australian code of practice for the care and use of animals for scientific purposes.

Mice were classified as "young adult" aged 3-6 months, or "aged" at 23-24 months. The single session of LI-rTMS group (total n=10 animals) had both young adult (4 male, 1 female) and aged adult animals (n=5 all male). The multiple sessions of LI-rTMS group (total n=5 animals) consisted of young adult animals only (3 males, 2 female).

Cranial window implantation

Animals were habituated to the animal facility for at least 7 days prior to cranial window implantation surgery. For cranial window imaging, we used a modified protocol from [20]. Briefly, animals were given pre-operative analgesia (buprenorphine, 0.1mg/kg, subcutaneous), anaesthetised with isoflurane and placed

98 in a stereotaxic frame. Local anaesthetic (5mg/kg bupivacaine) was infiltrated under
99 the scalp prior to incision and skin removal. A high-speed dental drill was used to
100 perform a 3mm craniotomy over the right primary motor cortex region (M1) likely
101 blending into the SS1 somatosensory region (window centred over +1mm anterior
102 from bregma, +2.5mm lateral to the midline). Artificial cerebrospinal fluid (ACSF) was
103 applied regularly to cool the bone during drilling. The exposed dura was left intact
104 and was gently cleaned with sterile gelfoam (Pfizer), soaked in ACSF.
105 Dexamethasone was applied topically to the dura (approximately 20µl of 4mg/ml
106 solution), as this has been shown to enhance window clearance [21]. A 5mm circular
107 glass coverslip was placed over the craniotomy, and the perimeter sealed with
108 Loctite 454 (a low-volatile, low-temperature curing cyanoacrylate gel). A titanium bar
109 with a threaded hole was glued onto the left side, opposite the window. The exposed
110 scalp and skin margin was sealed with dental acrylic (Heraeus). Animals recovered
111 over a 2–3-week period post-surgery before undergoing imaging.

112

113 *Multiphoton in vivo imaging*

114 *In vivo* two-photon laser scanning microscopy (2PLSM) was performed using a
115 custom-built upright laser scanning microscope (Scientifica) equipped with galvo-
116 galvo mirrors, a 20X water immersion lens (NA 1.0, Zeiss Plan-Apo) and a high-
117 sensitivity GaAsP non-descanned photomultiplier detector
118 (Hamamatsu). Femtosecond-pulsed infrared excitation was from a mode-locked Ti-
119 sapphire laser tuned to 910nm and equipped with group velocity dispersion
120 compensation (Mai Tai DeepSee, Spectra-Physics). Power delivered to the back
121 aperture was 20-90mW, depending on depth. This setup enabled us to image a good
122 cranial window to >1000µm into the cortex. Images were acquired with ScanImage
123 3.8.1 software (Vidrio Technologies, LLC) [22] incorporating the Navigator plugin.
124 Animals were anaesthetised during imaging using either isoflurane or injectable
125 anaesthetic (100mg/kg ketamine, 10mg/kg xylazine, intraperitoneal injection). The
126 titanium bar embedded in the acrylic cap during surgery was attached to a
127 customised brass clamp to maintain stability during imaging. Images of dendritic
128 arbours were captured from the upper 100µm of the cortex for the purposes of
129 quantification, and the neuron type (layer 2/3 or layer 5) was identified with deeper

imaging. Images were captured at 0.2μm/pixel resolution in the XY plane, with 1μm Z-steps. Dendritic arbours were selected on the basis of clarity and were not restricted to any particular position within the window. Repeat imaging of dendritic segments was carried out using vascular landmarks to locate the regions of interest.

Low intensity rTMS

Purpose built rodent specific coils (circular coil 8mm in diameter and height-see [2]) controlled by an arbitrary waveform generator (Agilent 335141B) connected to a bipolar power supply (Kepco BOP 100-4M) were used to administer the rTMS trains. The rTMS pulses were monophasic in shape (400μs rise time, dB/dT of 300T/s) which induced a peak magnetic field of 0.12T at the base of the coil. At this intensity, the peak sound intensity of the rTMS “clicks” are ~26dB SPL at the base of the coil [2] which is below the hearing thresholds previously reported for adult C57Bl6J mice [23]. Each stimulation session delivered 600 pulses of intermittent theta-burst stimulation (iTBS) [24] which contained pulse trains consisting of 3 pulses at 50Hz, repeated at 5Hz and delivered for 2s, with an inter-train interval of 8s (total stimulation time 192s).

LI-rTMS was delivered 3 hours after the end of each imaging session to allow for complete recovery from the anaesthesia, as anaesthesia during the delivery of rTMS has been shown to alter the effect of rTMS in the rodent brain [25, 26]. Stimulation was delivered to lightly restrained mice that were placed in a restraint bag with a breathing hole at one end (Able Scientific). The rTMS coil was positioned over the mouse cranium, such that the coil windings overlaid the cranial window, with the coil offset laterally to minimise direct stimulation of the motor cortex in the other hemisphere (i.e., the motor cortex without a cranial window). During stimulation, the coil was held directly on the restraint bag (~1mm distance from the base of the coil to the mouse cranium).

Imaging timeline

159 Imaging was separated into 3 time periods (summarised in Figure 1), (i) pre-
160 stimulation, (ii) +21 hours post-stimulation and (iii) +45 hours post-stimulation. For
161 both the single and multiple stimulation groups, pre-stimulation imaging consisted of
162 three imaging sessions conducted over 3 consecutive days separated by 24 hours to
163 capture baseline spine density and dynamics (rate of spine losses and gains). The
164 +21 hours post-stimulation timepoints were conducted 21 hours after each LI-rTMS
165 (i.e. once for the single session of LI-rTMS group or a total of four +21 hours post-
166 stimulation timepoints for the multiple stimulation group). A final imaging session was
167 conducted 24 hours after the last +21 hours post-stimulation period and represents
168 the +45 hours post-stimulation timepoint for both the single and multiple stimulation
169 groups.

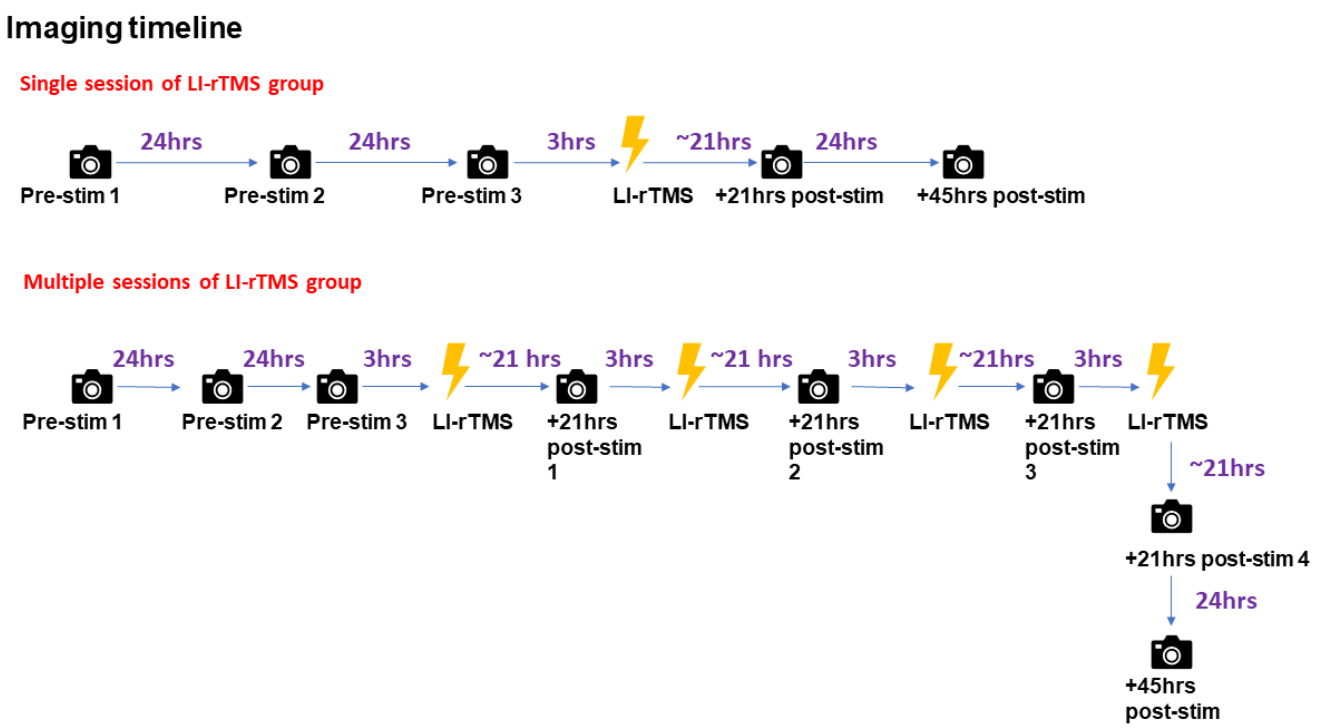

170

171 **Figure 1. Imaging timeline for the single and multiple sessions of LI-rTMS**
172 **groups.**

173 *Image annotation and spine analysis*

174 Captured stacks were screened for dendrite lengths that were suitable for spine
175 analysis. Although no minimum length was prescribed, only dendritic segments that
176 had at least 11 spines at the final pre-stimulation timepoint were included in the
177 analysis. This resulted in a total of 29 analysable dendritic segments for the single

stimulation group (pooled from 10 mice) and 15 analysable dendritic segments for the multiple stimulation group (pooled from 5 mice). Overlapping image stacks were montaged together using XUVTools software [27]. Image stacks were false coloured for depth in Fiji [28] and rotated in 3D to ensure that unique dendritic segments were identified. Where segments joined at a branch point, they were combined and considered to be a single segment. Segments were cropped and then annotated using Matlab scripts included with ScanImage (scim_spineAnalysis.m) to correlate spines across longitudinal time series [20, 22]. Spines were annotated by drawing a line from the centre of the dendritic backbone to the tip of the spine and were only annotated if present across two consecutive z-planes within the stack. Spines were then correlated across the timeseries and exported as spreadsheets of spine lengths where each column was a timepoint and each row corresponded to a single spine across the timeseries. For each dendritic segment, the width of the dendritic backbone was measured at five evenly spaced points along the segment and spine lengths were corrected by subtracting half the mean backbone width.

A custom R script (R core team, 2014) was used to analyse gains and losses, where the criterion for a spine being counted as present was set to 0.4μm (corresponding to two pixels protruding from the edge of the backbone). In addition, a spine had to reach a minimum of 0.6μm (three pixels) at some point along the timeseries, or the entire row was censored. Gains were therefore classified as when a spine went from absent (<0.4μm) to present (≥0.4μm), with loss being the inverse. Transient losses where the spine was absent for only a single timepoint before reappearing at the same location were checked manually. In all except a single case (out of more than 90 apparent transient loss events), these were found to be spurious, and were caused by poor image quality, or rotation of the spine around the backbone to project along the z-axis (detectable by an increase in the brightness of the backbone). All such transient loss events were reclassified as being present throughout. Following data curation and removal of dendritic arbours with insufficient spines, the dendritic arbours which were analysed statistically tallied (across all timepoints) 17 segments (total length 1807μm) with 2423 annotated spines in the young adult single stimulation group; 12 segments (total length 1691μm) with 1852 annotated spines in

210 the aged adult single stimulation group and 15 segments (total length 1586μm) with
211 2865 spines annotated in the young adult multiple stimulation group.

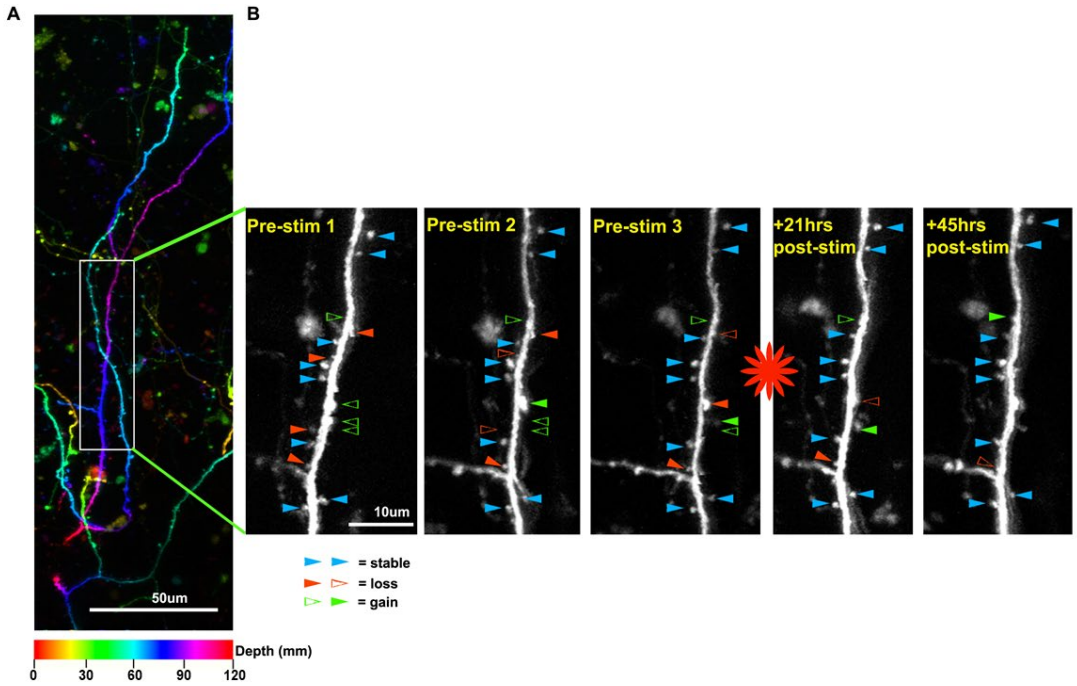

212

213 **Figure 2. Representative images of an analysed dendritic arbour from the**
214 **single session of LI-rTMS group.**

215 (A) Portion of a dendritic arbour, shown as a maximum projection of a 120μm
216 stack, false colour coded for depth. The colour scale along the bottom shows the
217 correspondence between hue and depth within the stack. Depth of an arbour within
218 the stack does not necessarily correspond to depth from the cortical surface, due to
219 the angle of capture. However, the colours do indicate the relative depths of
220 adjacent or overlapping dendrites. The rectangular box indicates a portion of the
221 annotated subregion shown in panel B).

222 (B) 60μm subregion of a single annotated dendrite from the single stimulation group
223 (total annotated length was 242μm), showing five sequential timepoints at 24hr
224 intervals. The red asterisk indicates LI-rTMS stimulation, occurring 3hrs after the
225 Pre-stim 3 image. Spines were annotated in MATLAB and quantitatively analysed
226 using custom R scripts, with the threshold for spine presence set to projection of
227 ≥0.4μm from the edge of the dendritic backbone. Spines over the time series were
228 classified as stable, lost or gained. Blue arrowheads indicate spines present
229 throughout (stable).

Filled red arrowheads indicate spines present that will be lost, with the point of loss shown as a hollow red arrowhead. Hollow green arrowheads indicate nascent spines that have not yet exceeded the threshold, with the solid green arrowhead indicating the point of gain.

Statistics

For statistical comparison, we compared the 3 time periods (pre-stimulation, +21hrs post-stimulation and +45hrs post-stimulation). Spine density represents the number of spines per µm measured at each imaging session/timepoint. The rate of spine losses and gains represents the number of new spines (per µm) gained or lost (per spine) *since* the last imaging session. The rate of spine losses cannot be calculated for the first pre-stimulation timepoint, as this timepoint provides the baseline counts of spines for each dendritic arbour. To facilitate comparison between gains and losses, we similarly excluded this timepoint for the analysis of gains.

Bayesian hierarchical generalized linear regression models were used to estimate ($\log_e$-) spine density and the rate of spine losses and gains at each 24-hour observation and the average rate (per 24-hour) within the 3 imaging periods (pre-stimulation, +21hrs post-stimulation, +45hrs post stimulation with LI-rTMS) for each stimulation group. Data were counts, therefore a Poisson distribution was assumed, with log-link function. The rate of spine losses per 24-hours was adjusted for the ($\log_e$-) spine count at the previous 24-hour observation of the same dendrite. The rate of spine gain per 24-hours was adjusted for dendritic length ($\log_e$-µm), as longer dendrites are likely to have more spines. Weakly regularizing student-t priors with 3 degrees of freedom (fat tails) were specified, expressing some scepticism that there was any difference in rate of gains or losses between observations or stimulation periods.

Given that the data in the single stimulation and multiple stimulation groups are identical in the way they are collected from the pre-stimulation period up to the first +21hrs post-stimulation observation (see Figure 1), a pooled analysis was run on this combined dataset to supplement our single stimulation analysis.

All statistical analysis was conducted in the R statistical computing environment (R Core Team, 2014). We used the R package 'brms' [29] to specify models using Hamiltonian Monte Carlo sampling in Stan [30]. Chain mixing and convergence was assessed using trace plots and R-hat statistics, and model fit was assessed using (graphical) posterior predictive checks. Estimated marginal means (averaged over age and/or layer) were computed using the 'emmeans' R package [31]. Marginal likelihoods were computed over 27×10^3 posterior samples (after a 3×10^3 iteration warmup). All code and data to reproduce the analysis will be accessible through online repositories (https://research-repository.uwa.edu.au/en/persons/alex-tang/datasets/ and https://eprints.utas.edu.au/).

We fitted 3-level models with random intercepts for dendritic segments nested within animal, with age and cell body location (layers 2/3 or 5) included as fixed effects. We report rate of gains per day, per micron, and rate of losses per day, per spine (lagged to the previous observation as described above). Uncertainty is expressed as 95% (posterior) credible intervals (CI). As we used an internal control design, our analysis (including hypothesis testing) estimates the dendritic spine dynamics at the population-level at the pre-, +21hrs post-stimulation and +45hrs post-stimulation time periods. Bayes Factors (BF- evidence ratios) are reported to aid in the interpretation of our results and we used the following BF cut-offs as evidence in favour of the alternative hypothesis [32].

- **BF = 1** - No evidence
- **1 < BF <= 3** - Anecdotal
- **3 < BF <= 10** - Moderate
- **10 < BF <= 30** - Strong
- **BF>100** – Extreme

Results

Single session of LI-rTMS (young adult and aged mice)

Density

Compared to pre-stimulation (0.216 spines μm^{-1}, 95%CI 0.149, 0.284, averaged over layer and age, n=29 dendritic segments from 10 mice) there was anecdotal evidence for a decrease in spine density at +21hrs post-stimulation (0.213 spines μm^{-1}, 95%CI 0.146, 0.282, BF=1.78). In contrast, there was strong evidence for a decrease in the mean dendritic spine density at +45hrs post-stimulation (0.201 spines μm^{-1}, 95%CI 0.137, 0.265, BF =18.2, see Figure 3A). Further analysis showed anecdotal evidence for a greater effect of LI-rTMS on dendritic spine density in young adults (n=5) compared to aged animals (n=5) (BF=1.5).

Rate of spine loss

Compared to pre-stimulation (0.228 $spine^{-1}$, 95%CI 0.156, 0.315, averaged over layer and age), there was strong evidence for an increase in the mean rate of spine losses following LI-rTMS at +21hrs post-stimulation (0.262 $spine^{-1}$, 95%CI 0.173, 0.361, BF =13.4) but not at +45hrs post-stimulation (0.227 $spine^{-1}$, 95%CI 0.151, 0.313, BF=1.1, see Figure 3C). In addition, there was strong evidence for a greater rate of spine losses at +21 and compared to +45hrs post-stimulation (BF=10.3), further suggesting that there was an increase in the rate of spine loss following LI-rTMS that resolves by +45hrs post-stimulation. Analysis of age showed moderate evidence for a greater increase in the rate of spine losses in young adult animals compared to aged adult animals (BF=4.2).

Rate of spine gain

Compared to pre-stimulation (0.046 spines μm^{-1}, 95%CI 0.035, 0.058, averaged over layer and age), there was anecdotal evidence of an increase in the rate of spine gain following LI-rTMS +21hrs post-stimulation (0.048 spines μm^{-1}, 95%CI 0.035, 0.06, averaged over layer and age, BF = 2.0, see Figure 3E). In contrast, there was extreme evidence for a decrease in the rate of spine gain at +45hrs post-stimulation (0.034 spines μm^{-1}, 95%CI 0.025, 0.044, averaged over layer and age, pre-stimulation> +45hrs post-stimulation: BF = 564.4, +45hrs post-stimulation< +21hrs post-stimulation: BF = 661.6). There was anecdotal evidence for a greater change in the rate of spine gain between young adult and aged animals (BF=0.9).

319

320 **Multiple sessions of LI-rTMS (young adult mice)**

321 *Density*

322 Compared to the pre-stimulation period (0.216 spines μm^{-1}, 95%CI 0.149, 0.284,
323 n=15 dendritic segments from 5 mice, averaged over layer), there was anecdotal
324 evidence for a decrease in the mean density of dendritic spines following LI-rTMS at
325 the +21hrs post-stimulation timepoints (averaged over the 4 +21hrs post-stimulation
326 timepoints, 0.213 spines μm^{-1}, 95%CI 0.146, 0.282, BF = 1.8, see Figure 3B) and at
327 +45hrs post-stimulation (0.220 spines μm^{-1}, 95%CI 0.137, 0.265, BF = 2.4). In
328 addition, there was anecdotal evidence for an increase in density between the
329 +21hrs post-stimulation timepoints and +45hrs post-stimulation (BF=4.2).

330 *Rate of spine loss*

331 Compared to pre-stimulation (0.166 $spine^{-1}$, 95%CI 0.116, 0.219, averaged over
332 layer), there was strong evidence for an increase in the mean rate of spine losses at
333 the +21hrs post-stimulation timepoints (averaged over the 4 +21hrs post-stimulation
334 timepoints 0.199 $spine^{-1}$, 95%CI 0.146, 0.255, BF= 20.4, see Figure 3D) but not at
335 +45hrs post-stimulation (0.175 $spine^{-1}$, 95%CI 0.111, 0.240, BF=1.6).

336 *Rate of spine gain*

337 Compared to pre-stimulation (0.057 spines μm^{-1}, 95%CI 0.014, 0.109, averaged over
338 layer), there was anecdotal evidence for a decrease in the mean rate of spine gain at
339 the +21hrs post-stimulation timepoints (averaged over the 4 +21hrs post-stimulation
340 timepoints +0.059 spines μm^{-1}, 95%CI 0.016, 0.115, BF= 1.9, see Figure 3F).
341 Following LI-rTMS, there was moderate evidence for a decrease in the rate of spine
342 gain at +45hrs post-stimulation (0.050 spines μm^{-1} 95%CI 0.013, 0.098, BF = 3.5).

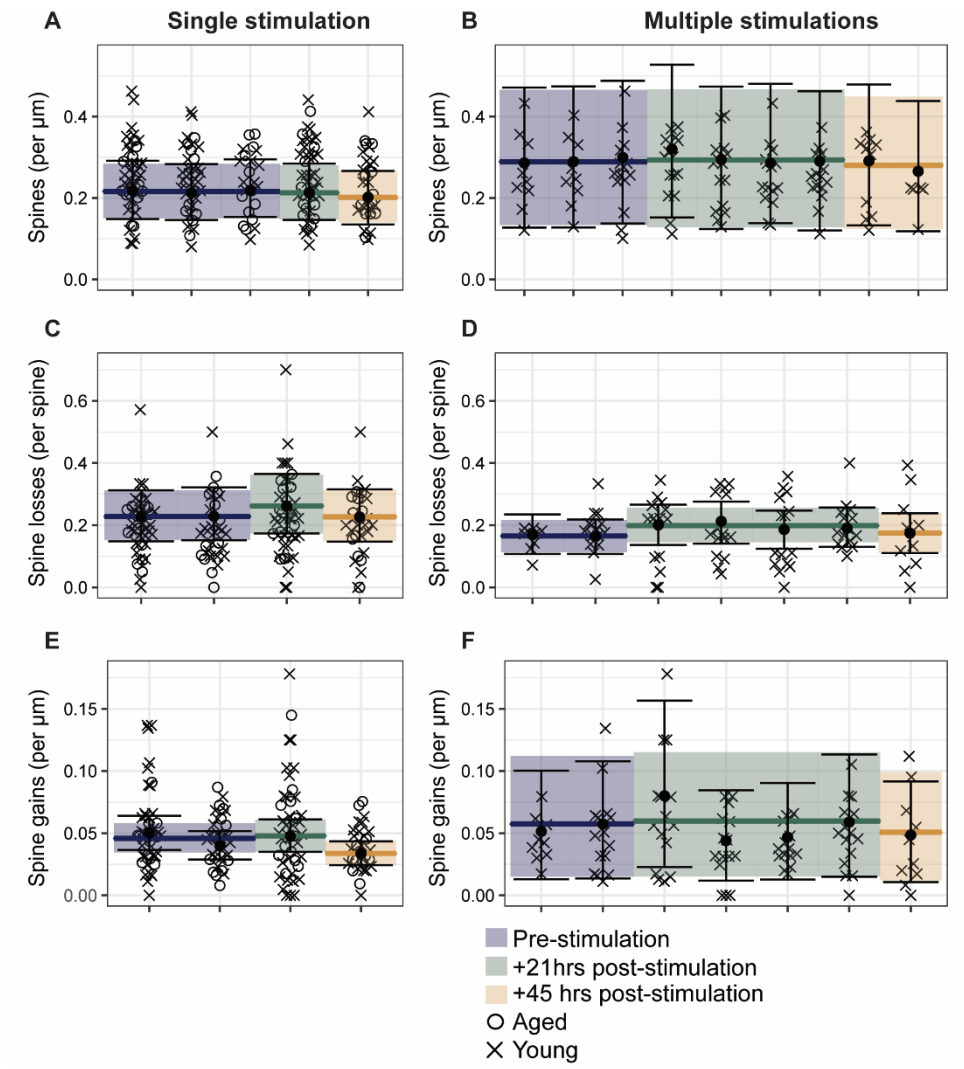

Figure 3: Single (left side) and multiple sessions of LI-rTMS (right side) drive structural synaptic plasticity in pyramidal neurons of the motor cortex.

(A and B) Analysis of dendritic spine density showed strong evidence for a decrease in the mean dendritic spine density +45hrs post a single session of LI-rTMS, compared to pre-stimulation.

(C and D) Analysis of the rate of dendritic spine losses showed strong evidence for an increase in the mean rate of spine losses +21hrs post-stimulation in both the single and multiple sessions of LI-rTMS groups compared to pre-stimulation.

(E and F) Analysis of the rate of dendritic spine gains showed strong evidence for a decrease in the mean rate of dendritic spine gains +45hrs post a single session of LI-rTMS compared to pre-stimulation.

355 Data are shown as the aggregate means (solid-coloured lines) for each time period
356 (pre-stimulation=blue, +21hrs post-stimulation=green, +45hrs post-
357 stimulation=orange) overlaid on the mean (•) at each imaging observation. Error
358 bars represent the 95% **credible intervals** for each timepoint, whereas the shaded
359 boxes represent the 95% credible intervals for each time period. Each data point
360 represents data from an individual dendritic arbour with data from young (o) and
361 aged (x) animals.

362

363 **Pooled analysis of single and multiple stimulation data (from pre-stimulation**
364 **to the first +21hrs post-stimulation timepoint)**

365 As the single and multiple stimulation groups are identical experimentally, to the first
366 +21hrs post-stimulation imaging timepoint (i.e., up to +21hrs post a single
367 stimulation), we pooled the data from both groups up until this point to supplement
368 our single stimulation analysis.

369 *Density*

370 Increasing the sample size in the pooled analysis (total n=44 dendritic segments
371 from 26 arbours, from 15 mice) showed anecdotal evidence for an increase in the
372 mean dendritic spine density +21hrs post a single session of LI-rTMS (0.229 spines
373 μm^{-1}, 95%CI 0.173, 0.288) compared to pre-stimulation (0.223 spines μm^{-1}, 95%CI
374 0.171, 0.284, BF = 2.1, see Supplementary Figure 1A).

375 *Rate of spine loss*

376 Pooled analysis showed strong evidence of an increase in the rate of spine losses at
377 +21hrs post a single session of LI-rTMS (0.238 $spine^{-1}$, 95% CI 0.150, 0.263)
378 compared to pre-stimulation (0.204 $spine^{-1}$, 95% CI 0.174, 0.307, BF=34.9, see
379 Supplementary Figure 1B).

380

381 *Rate of spine gains*

Pooled analysis showed strong evidence (BF=35.0, see Supplementary Figure 1C) for an increase in the rate of spine gain at the +21hrs post a single session of LI-rTMS (0.053 spines μm^{-1} 95%CI 0.035, 0.057) compared to pre-stimulation (0.045 spines μm^{-1} 95%CI 0.039, 0.066).Given that this result was not evident in the single stimulation analysis, this suggests that this effect is not as robust as the change seen in spine losses, as it could only be detected by increasing the sample size Further analysis of the pooled data did not indicate that animals in the multiple stimulation group had a greater increase in gains during the first +21hrs post-stimulation period compared to the animals in the single stimulation group (see Supplementary Material).

393 **Table 1. Summary of results after LI-rTMS (i.e., post-stimulation time points**
394 **compared to pre-stimulation).** The direction of change (increased/decreased) is
395 indicated only for results with a BF≥10 (i.e., with ≥strong evidence of a change).
396 NOTE: "Age" is not included in the table as it was investigated in the single
397 stimulation group only and did not show strong evidence for any spine measure.
398 Pooled analysis encompasses +21hrs post-stimulation time points only.

399

	Dendritic spine density		**Rate of dendritic spine losses**		**Rate of dendritic spine gains**	
	+21 hours post-stim	+45 hours post-stim	+21 hours post-stim	+45 hours post-stim	+21 hours post-stim	+45 hours post-stim
Single session of LI-rTMS	-	↓	↑	-	-	↓
	BF=1.78	BF=18.2	BF=13.4	BF=1.1	BF=2.0	BF=564.4
Multiple sessions of LI-rTMS	-	-	↑	-	-	-
	BF=1.8	BF=2.4	BF=20.4	BF=1.6	BF=1.9	BF=3.5
Pooled analysis up to first +21hrs post-stimulation timepoint	-		↑		↑	
	BF=2.1		BF=34.9		BF=35.0	

400

401 **Discussion**

402 To our knowledge, this is the first *in vivo* study to provide direct evidence that rTMS,
403 irrespective of intensity, drives structural synaptic plasticity in the motor cortex.
404 Following a single session of LI-rTMS, there was an increase to the rate of dendritic
405 spine losses (present at +21hrs post-stimulation) and a long-lasting decrease in

406 dendritic spine density and to the rate of dendritic spine formation (present at +45hrs
407 post-stimulation) which did not differ between young and aged animals (see Figure
408 3). Surprisingly, multiple days/sessions of LI-rTMS did not have a cumulative effect
409 or longer lasting effect on structural plasticity compared to a single session of LI-
410 rTMS but instead maintained the more acute effects induced by a single LI-rTMS
411 session (increased rate of spine losses at +21hrs post-stimulation) which returned to
412 baseline values by +45hrs after the last LI-rTMS session.

413

414 Given that previous high intensity rTMS studies in humans have shown age-related
415 differences in rTMS-induced plasticity in other measures of neural plasticity (motor
416 evoked potentials and the default mode network) with the iTBS protocol [12, 13], we
417 might have expected similar results in our study. However, we failed to find strong
418 evidence of a difference between young adult and aged animals in the structural
419 plasticity of dendritic spines induced by a single session of LI-rTMS. This may be
420 explained by the absence of age-dependent differences in dendritic spine properties
421 pre-stimulation, such that LI-rTMS modulated both the young and aged brain as they
422 did not differ in the amounts of synaptic connectivity and remodelling capacity prior
423 to stimulation. Interestingly, these results are in direct contrast to the work of
424 Davidson et al., who reported age-dependent differences in pyramidal neuron
425 dendritic spine density and dynamics in the forelimb region of the motor cortex in
426 Thy1-GFP mice [10]. Specifically, in both our young and aged animals, the mean
427 dendritic spine density and rate of spine *gains* in the pre-stimulation period was
428 approximately half of that reported by Davidson et al., whereas the rate of spine
429 *losses* from our young adults was almost twice as large. In addition to several
430 methodological differences that may explain these contrasting findings, a key point of
431 difference between our studies was that our cranial windows were centred more
432 anterior relative to bregma to that used in Davidson et al. Therefore, while we did not
433 find age-dependent effects on baseline or LI-rTMS induced spine plasticity in the
434 area of the motor cortex we imaged, it's possible that such differences do occur,
435 depending on the anatomical region imaged or circuit stimulated.

436

In young adult mice, we have previously shown that 10 daily sessions of LI-rTMS (with the same 600 pulses of iTBS protocol) to the motor cortex paired with skilled motor training improves motor behaviour and the rate of learning [3]. In that study, our behavioural analysis suggested that multiple sessions of LI-rTMS maintained the transient effects induced by a single stimulation. Similarly, repeated blocks of high intensity iTBS within a single stimulation session to the rat barrel cortex was shown to have a cumulative effect on cortical activity [33]. Interestingly, multiple sessions of LI-rTMS maintained the initial structural plasticity induced by LI-rTMS, with both groups showing an increase in the rate spine losses at the +21hrs post-stimulation timepoint (pooled analysis- see supplementary Figure 1). However, the effects of multiple sessions were shorter lasting (+21hrs post-stimulation) compared to a single session which also showed decreased spine density and rate of spine gains at the +45hrs post-stimulation timepoint. While it is unclear why a single-session of LI-rTMS had longer lasting effects on structural plasticity than multiple-sessions, the net changes observed with both groups suggest a common outcome of refinement in synaptic connectivity as an underlying mechanism of LI-rTMS-induced plasticity.

This is the first demonstration, to our knowledge, that LI-rTMS has delayed effects on neural plasticity, as our previous work has shown that LI-rTMS (using the iTBS protocol) drives acute changes to motor behaviour [3] and neuronal excitability [1]. While further investigation is needed to determine the functional consequences of structural plasticity induced with LI-rTMS, we suggest that the refinement in synaptic connectivity induced may promote neural plasticity, by removing or preventing redundant synaptic connections, thereby producing a more efficient neural circuit. This is consistent with the use of LI-rTMS (0.012T) in ephrin-A2A5-/- mice showing that LI-rTMS reorganises abnormal circuitry by removing aberrant connections [34, 35].This delayed form of LI-rTMS induced structural plasticity in the motor cortex may work in tandem with, or be a result of the immediate effects of LI-rTMS, such that the acute changes in neuronal excitability enhance motor behaviour which is later supported by the delayed refinement/pruning of the neural circuitry. However, future studies combining LI-rTMS with motor training and *in vivo* imaging is needed to confirm our theory.

The use of rodent-specific coils offered us the advantage of delivering focal stimulation (e.g. restricting stimulation to one motor cortex) but at the expense of stimulation intensity [2]. Therefore, while we have shown that LI-rTMS (i.e. subthreshold stimulation) induces synaptic plasticity, it remains unknown what effect high intensity/suprathreshold rTMS has on structural synaptic plasticity *in vivo*. Investigating such changes in a mouse model is technically challenging as “small” commercial coils (e.g. 25mm figure of 8 coils) stimulate the entire brain [36]. In addition, despite promising improvements in rodent-specific TMS coils [37], there are currently no rTMS coils appropriately sized for the mouse brain that can deliver high intensity rTMS, due to the thermal stress induced with each pulse [2, 38], particularly at high stimulation frequencies such as iTBS. As a result, characterising structural synaptic plasticity with *in vivo* imaging following high intensity rTMS may be more practical in a rat model, where commercial coils can be used with some degree of focality [26, 39, 40].

Despite the extremely low sound generation (<26dBL sound pressure) produced by our rodent coils during rTMS, a limitation of our study is the absence of a sham stimulation group. While internal controls/ comparisons to pre-stimulation measures are commonly used in human rTMS studies (e.g., motor evoked potential properties normalised to pre-stimulation values), we cannot rule out the possibility that our results were influenced by factors outside of LI-rTMS such as daily anaesthesia. However, given that we did not observe a consistent change over time (e.g., a change in dendritic spine density that increased over time) or consistent changes between the stimulation groups (e.g., a change in a dendritic spine property that was seen at the 5th imaging session in both the single and multiple stimulation groups), repeated anaesthesia is unlikely to have been a significant factor.

In conclusion, our results show that LI-rTMS drives structural synaptic plasticity in the mouse motor cortex. These findings uncover structural synaptic plasticity as a key mechanism of LI-rTMS induced neural plasticity and more broadly, highlights the ability of rTMS to alter synaptic connectivity in the brain.

Acknowledgements

The authors thank Claire Hadrill for her assistance with the initial spine annotations and Dr Saied Mehrkanoon for assistance with the modification and re-generation of the MATLAB scripts used for spine annotations. This project was funded by the National Health and Medical Research Council (NHMRC - APP1050261). JR was supported by research fellowships from the NHMRC (APP1002258) and Multiple Sclerosis Western Australia. MRH was supported by research fellowships from the Australian Research Council (DE120100729 and FT150100406). AT was supported by doctoral scholarship from the Australian Government, the Bruce and Betty Green Foundation and post-doctoral funding from the Raine Medical Research Foundation (RPG06-20).

References

1. Tang AD, Hong I, Boddington LJ, Garrett AR, Etherington S, Reynolds JN, et al. Low-intensity repetitive magnetic stimulation lowers action potential threshold and increases spike firing in layer 5 pyramidal neurons in vitro. Neuroscience. 2016;335:64-71.
2. Tang AD, Lowe AS, Garrett AR, Woodward R, Bennett W, Canty AJ, et al. Construction and evaluation of rodent-specific rTMS coils. Front Neural Circ. 2016;10:47.
3. Tang AD, Bennett W, Hadrill C, Collins J, Fulopova B, Wills K, et al. Low intensity repetitive transcranial magnetic stimulation modulates skilled motor learning in adult mice. Sci Rep. 2018;8(4016).
4. Cullen CL, Senesi M, Tang AD, Clutterbuck MT, Auderset L, O'Rourke ME, et al. Low-intensity transcranial magnetic stimulation promotes the survival and maturation of newborn oligodendrocytes in the adult mouse brain. Glia. 2019;67(8):1462-77.
5. Cullen CL, Pepper RE, Clutterbuck MT, Pitman KA, Oorschot V, Auderset L, et al. Periaxonal and nodal plasticities modulate action potential conduction in the adult mouse brain. Cell Rep. 2021;34(3):108641.
6. Thickbroom GW. Transcranial magnetic stimulation and synaptic plasticity: experimental framework and human models. Exp Brain Res. 2007;180(4):583-93.

532 7. Tang A, Thickbroom G, Rodger J. Repetitive transcranial magnetic stimulation
533 of the brain: mechanisms from animal and experimental models. Neuroscientist.
534 2017;23(1):82-94.
535 8. Landfield PW, McGaugh JL, Lynch G. Impaired synaptic potentiation
536 processes in the hippocampus of aged, memory-deficient rats. Brain Res.
537 1978;150(1):85-101.
538 9. Pinho J, Vale R, Batalha VL, Costenla AR, Dias R, Rombo D, et al. Enhanced
539 LTP in aged rats: Detrimental or compensatory? Neuropharmacology. 2017;114:12-
540 9.
541 10. Davidson AM, Mejía-Gómez H, Jacobowitz M, Mostany R. Dendritic spine
542 density and dynamics of layer 5 pyramidal neurons of the primary motor cortex are
543 elevated with aging. Cereb Cortex. 2020;30(2):767-77.
544 11. Todd G, Kimber TE, Ridding MC, Semmler JG. Reduced motor cortex
545 plasticity following inhibitory rTMS in older adults. Clin Neurophysiol.
546 2010;121(3):441-7.
547 12. Opie GM, Vosnakis E, Ridding MC, Ziemann U, Semmler JG. Priming theta
548 burst stimulation enhances motor cortex plasticity in young but not old adults. Brain
549 Stimul. 2017;10(2):298-304.
550 13. Abellaneda-Pérez K, Vaqué-Alcázar L, Vidal-Piñeiro D, Jannati A, Solana E,
551 Bargalló N, et al. Age-related differences in default-mode network connectivity in
552 response to intermittent theta-burst stimulation and its relationships with maintained
553 cognition and brain integrity in healthy aging. NeuroImage. 2019;188:794-806.
554 14. Vlachos A, Müller-Dahlhaus F, Rosskopp J, Lenz M, Ziemann U, Deller T.
555 Repetitive magnetic stimulation induces functional and structural plasticity of
556 excitatory postsynapses in mouse organotypic hippocampal slice cultures. J
557 Neurosci. 2012;32(48):17514-23.
558 15. Lenz M, Platschek S, Priesemann V, Becker D, Willems LM, Ziemann U, et al.
559 Repetitive magnetic stimulation induces plasticity of excitatory postsynapses on
560 proximal dendrites of cultured mouse CA1 pyramidal neurons. Brain Struct Funct.
561 2015;220(6):3323-37.
562 16. Lenz M, Galanis C, Müller-Dahlhaus F, Opitz A, Wierenga CJ, Szabó G, et al.
563 Repetitive magnetic stimulation induces plasticity of inhibitory synapses. Nat
564 Commun. 2016;7:10020.

565 17. Xu T, Yu X, Perlik AJ, Tobin WF, Zweig JA, Tennant K, et al. Rapid formation
566 and selective stabilization of synapses for enduring motor memories. Nature.
567 2009;462(7275):915-9.
568 18. Fu M, Yu X, Lu J, Zuo Y. Repetitive motor learning induces coordinated
569 formation of clustered dendritic spines in vivo. Nature. 2012;483(7387):92-5.
570 19. Feng G, Mellor RH, Bernstein M, Keller-Peck C, Nguyen QT, Wallace M, et al.
571 Imaging neuronal subsets in transgenic mice expressing multiple spectral variants of
572 GFP. Neuron. 2000;28(1):41-51.
573 20. Holtmaat A, Bonhoeffer T, Chow DK, Chuckowree J, De Paola V, Hofer SB, et
574 al. Long-term, high-resolution imaging in the mouse neocortex through a chronic
575 cranial window. Nat Protoc. 2009;4(8):1128-44.
576 21. Park K, You J, Du C, Pan Y. Cranial window implantation on mouse cortex to
577 study microvascular change induced by cocaine. Quant Imaging Med Surg.
578 2014;5(1):97-107.
579 22. Pologruto TA, Sabatini BL, Svoboda K. ScanImage: Flexible software for
580 operating laser scanning microscopes. Biomed Eng Online. 2003;2(1):13.
581 23. Yu Y-F, Zhai F, Dai C-F, Hu J-J. The relationship between age-related
582 hearing loss and synaptic changes in the hippocampus of C57BL/6J mice. Exp
583 Gerentol. 2011;46(9):716-22.
584 24. Huang Y-Z, Edwards MJ, Rounis E, Bhatia KP, Rothwell JC. Theta burst
585 stimulation of the human motor cortex. Neuron. 2005;45(2):201-6.
586 25. Gersner R, Kravetz E, Feil J, Pell G, Zangen A. Long-term effects of repetitive
587 transcranial magnetic stimulation on markers for neuroplasticity: differential
588 outcomes in anesthetized and awake animals. J Neurosci. 2011;31(20):7521. doi:
589 10.1523/JNEUROSCI.6751-10.2011.
590 26. Sykes M, Matheson NA, Brownjohn PW, Tang AD, Rodger J, Shemmell JBH,
591 et al. Differences in motor evoked potentials induced in rats by transcranial magnetic
592 stimulation under two separate anesthetics: implications for plasticity studies. Front
593 Neural Circ. 2016;10(80).
594 27. Emmenlauer M, Ronneberger O, Ponti A, Schwarb P, Griffa A, Filippi A, et al.
595 XuvTools: free, fast and reliable stitching of large 3D datasets. J Microsc.
596 2009;233(1):42-60.

597 28. Schindelin J, Arganda-Carreras I, Frise E, Kaynig V, Longair M, Pietzsch T, et
598 al. Fiji: an open-source platform for biological-image analysis. Nat Methods.
599 2012;9(7):676-82.
600 29. Bürkner P-C. Advanced Bayesian multilevel modeling with the R package
601 brms. R J. 2018;10(1).
602 30. Stan-development-team. RStan: The R interface to Stan. R package version
603 2.19.3. http://mc-stan.org/ ed2020.
604 31. Lenth R, Singmann H, Love J, Buerkner P, Herve M. Emmeans: Estimated
605 marginal means, aka least-squares means. R package version. 2018;1(1):3.
606 32. Jeffreys H. The Theory of Probability. Third Edition ed: Oxford University
607 Press; 1961.
608 33. Thimm A, Funke K. Multiple blocks of intermittent and continuous theta-burst
609 stimulation applied via transcranial magnetic stimulation differently affect sensory
610 responses in rat barrel cortex. J Phsyiol. 2015;593(4):967-85.
611 34. Rodger J, Mo C, Wilks T, Dunlop SA, Sherrard RM. Transcranial pulsed
612 magnetic field stimulation facilitates reorganization of abnormal neural circuits and
613 corrects behavioral deficits without disrupting normal connectivity. FASEB J.
614 2012;26(4):1593-606.
615 35. Makowiecki K, Harvey AR, Sherrard RM, Rodger J. Low-intensity repetitive
616 transcranial magnetic stimulation improves abnormal visual cortical circuit
617 topography and upregulates BDNF in mice. J Neurosci. 2014;34(32):10780.
618 36. Alekseichuk I, Mantell K, Shirinpour S, Opitz A. Comparative modeling of
619 transcranial magnetic and electric stimulation in mouse, monkey, and human.
620 Neuroimage. 2019;194:136-48.
621 37. Meng Q, Jing L, Badjo JP, Du X, Hong E, Yang Y, et al. A novel transcranial
622 magnetic stimulator for focal stimulation of rodent brain.
623 38. Weissman JD, Epstein CM, Davey KR. Magnetic brain stimulation and brain
624 size: relevance to animal studies. Electroencephalogr Clin Neurophysiol.
625 1992;85(3):215-9.
626 39. Rotenberg A, Muller PA, Vahabzadeh-Hagh AM, Navarro X, López-Vales R,
627 Pascual-Leone A, et al. Lateralization of forelimb motor evoked potentials by
628 transcranial magnetic stimulation in rats. Clin Neurophysiol. 2010;121(1):104-8.

40. Murphy SC, Palmer LM, Nyffeler T, Müri RM, Larkum ME. Transcranial magnetic stimulation (TMS) inhibits cortical dendrites. eLife. 2016;5:e13598. doi: 10.7554/eLife.13598.